

Proton Decay of the Isobaric Analogs of the Ground States of ^{206}Pb , ^{207}Pb , ^{208}Pb , and $^{209}\text{Bi}^\dagger$

G. M. Crawley and P. S. Miller

Cyclotron Laboratory, Michigan State University, East Lansing, Michigan 48823

(Received 30 December 1971)

The $(p, n\bar{p})$ reaction has been measured on the lead isotopes ^{206}Pb , ^{207}Pb , and ^{208}Pb and on ^{209}Bi . Coulomb-energy differences are extracted from the positions of the \bar{p} peaks. Proton decay widths are also obtained and compared with values from resonance experiments and with a previous value from $^{209}\text{Bi}(p, n\bar{p})$.

I. INTRODUCTION

The $(p, n\bar{p})$ reaction¹ has been observed in a number of nuclei from ^{67}Zn to ^{209}Bi .²⁻⁴ This reaction allows one to study the position and width of the isobaric analog state⁵ (IAS) populated in the (p, n) reaction without the difficulty of neutron detection. In principle, proton decay widths of the IAS can also be measured if the (p, n) cross section leading to the IAS is known. However, for nuclei in the lead region, decays to more than one final state are observed and therefore *relative* proton decay widths can be obtained independent of the (p, n) cross section. These same widths can also be obtained by resonant elastic and inelastic proton scattering on a target with one less neutron than is required for the $(p, n\bar{p})$ experiments. This illustrates another feature of the $(p, n\bar{p})$ reaction. Since it can be used to study nuclei that cannot be reached by resonance reactions on stable nuclei, it provides complementary information. For example, the IAS studied by $^{208}\text{Pb}(p, n\bar{p})$ can only be reached by a resonance reaction on the unstable nucleus ^{205}Pb .

Earlier measurements of the partial widths for decay of the IAS in ^{208}Bi had shown agreement between the resonance measurements and the $^{208}\text{Pb}(p, n\bar{p})$ experiment. However, measurements of the $^{209}\text{Bi}(p, n\bar{p})$ reaction gave a relative proton width for the IAS in ^{209}Po which differed significantly from the measurements in ^{208}Bi . This was surprising, since one would not expect the extra $h_{9/2}$ proton in the ^{209}Bi parent nucleus to make a significant difference to the proton decay widths. This discrepancy encouraged us to repeat the $^{208}\text{Pb}(p, n\bar{p})$ experiment as a check on the earlier measurements. In addition, measurements on ^{206}Pb and ^{207}Pb were also made, and the $^{209}\text{Bi}(p, n\bar{p})$ experiment was repeated.

II. EXPERIMENT

The experimental arrangement is similar to that

discussed in an earlier paper on ^{209}Bi .⁴ The reactions were studied at many energies from 21.3 to 35 MeV using the proton beam from the Michigan State University isochronous cyclotron. A standard counter telescope of cooled silicon detectors was used to detect the protons. Deuteron spectra were taken simultaneously, since the (p, d) reaction produces the same final nuclei and therefore provides an energy calibration. The deuteron resolution also gives an accurate check of the target thickness measurement. Spectra were taken at many angles to avoid contaminant peaks and to check kinematic effects. Various targets of thickness from 1 to 6 mg/cm² were used in the experiment.

Kinematic effects are very important in a discussion of the $(p, n\bar{p})$ reaction, since both the energy of the detected protons and the shape of the peak depend on the angle of detection. This dependence arises from the angular distribution of the recoiling nuclei and therefore depends on the (p, n) angular distribution, which changes as the bombarding energy is changed. Calculations of both of these effects for model (p, n) angular distributions were shown in a previous paper.⁴ Even for heavy nuclei the shift and the broadening of the peak is significant and must be taken into account when extracting widths, even though the intrinsic width of the analog state is large (>200 keV) and dominates the observed width of the peak. A calculation for the energy shift of the \bar{p} peak using a measured (p, n) angular distribution⁶ at 24.8 MeV is shown in Fig. 1 together with the experimental kinematic shifts for ^{209}Bi . The Bi target is quite free of impurities and allows a more complete angular distribution to be obtained than could be done for lead. Line-shape calculations at various angles are shown in Fig. 2 for the same (p, n) angular distribution. A Lorentzian function with a 220-keV total width is also shown on the same scale. The line shapes fold in such a way that the total observed full width at half maximum (FWHM)

is very close to the sum of squares of the individual widths. Also, the tails of the peak are comparatively unchanged because the kinematic shapes cut off rather sharply, in contrast to the Lorentzian. Except around 90° , the kinematic broadening is considerably less than the observed total widths. In our analysis the calculated line shapes from both target thickness and kinematic effects were folded with the theoretical line shape in the fitting program from which the proton decay widths are obtained. This point has been stressed, since there is an apparent problem with the observed widths, so it is therefore important to eliminate possible sources of broadening.

III. COULOMB ENERGIES

The Coulomb-energy difference measured by ${}^A\text{Pb}(p, n\bar{p})$ is given by the expression

$$E_C = E_p(\text{c.m.}) + B_n({}^A\text{Pb}),$$

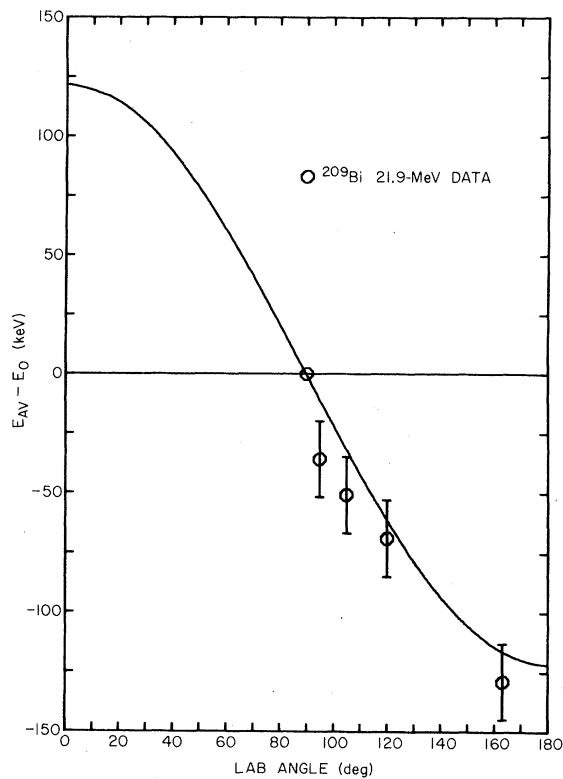


FIG. 1. Laboratory centroid energy of the decay proton group from the $(\pi h_{9/2}, \nu p_{1/2}^{-1})$ multiplet in the ${}^{209}\text{Bi}(p, n\bar{p})$ reaction. Experimental energies are measured relative to the value at 90° , which is also the value that would be obtained if the IAS decayed at rest (E_0). The curve is calculated using the angular distribution for the ${}^{208}\text{Pb}(p, n)$ charge-exchange cross section at 24.8 MeV from Ref. 6. This may be somewhat different from the unmeasured ${}^{209}\text{Bi}(p, n)$ distribution at 21.9 MeV, which should be used in the comparison with the data shown.

where $E_p(\text{c.m.})$ is the energy of the emitted proton in the center-of-mass system [$E_p(\text{c.m.}) = E_p(\text{lab})A/(A-1)$] and $B_n({}^A\text{Pb})$ is the binding energy of the last neutron in the Pb isotope of atomic mass A .

There are a number of factors which affect the accuracy of the measurement of the decay proton energy. While the absolute energy of the decay protons from the analog state is independent of the bombarding energy, the absolute calibration of the detector depends upon the calibration of the energy-analysis magnets in the beam-transport system. Calibration runs using a Mylar target were taken before and after most \bar{p} runs to calibrate the detector. The other main factors apart from the kinematics discussed above which affect the Coulomb-energy measurements are target thickness, the calibration of the detector, and the extraction of the centroid of the \bar{p} peak. The absolute calibration does not enter significantly into the relative measurements in this laboratory but will affect comparisons with measurements made elsewhere.

The target thickness was usually determined from α -gauge measurements and checked by measuring the resolution of the deuteron peaks, the width of which is predominantly due to the target thickness. The results of these two techniques were consistent and generally contribute less than 10 keV to the uncertainty in the measured Cou-

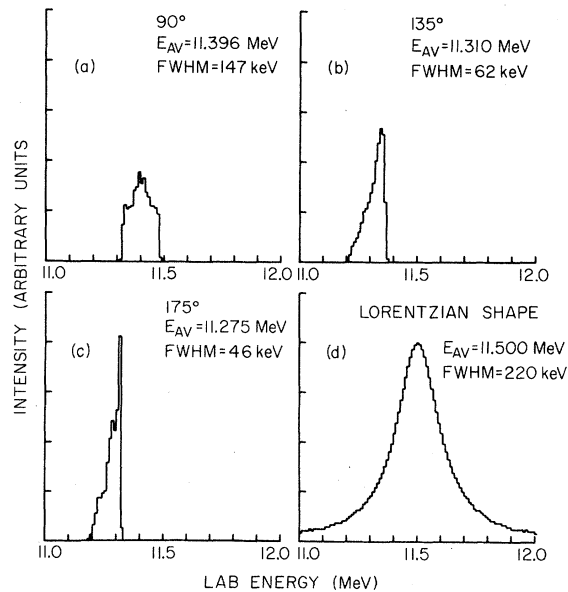


FIG. 2. Calculated line shapes. Sections (a), (b), and (c) are pure kinematic shapes for ${}^{208}\text{Pb}(p, n\bar{p})$ assuming negligible intrinsic widths and target broadening. The Lorentzian function in (d) corresponds to a total width Γ of 220 keV. The centroid energy and full width at half maximum are indicated for each peak.

lomb energies. For the best runs the errors from calibration of the detector and the determination of the centroid were each about 20 keV, but for runs with poorer statistics the uncertainties were as large as 50 keV.

Many independent runs were taken, particularly for ^{206}Pb and ^{209}Bi . For each of these, the final value is the weighted mean of 13 separate runs. Four and five independent runs were averaged for ^{207}Pb and ^{206}Pb , respectively, and the errors are correspondingly larger.

A new calibration of the beam-analysis magnets allowed a better calibration of the detector which is probably accurate to ± 10 keV.⁷ This compares with the old uncertainty of 50 keV. Remeasurement of the $\text{Bi}(p, n\bar{p})$ Coulomb energy using the new calibration gave a new value of 18.991 MeV, somewhat higher than the earlier value but consistent within the uncertainties quoted in the previous paper.⁴

The results of the Coulomb-energy measurements are shown in Table I and are also plotted together with the results of other Coulomb-energy measurements in the Pb isotopes⁸⁻¹² in Fig. 3. The graph shows differences between the data and the predictions of Long *et al.*,¹³ who obtained a formula for the Coulomb energy based on a charged-sphere model for the nucleus. The coefficients were determined from a fit to measurements in nuclei lighter than the lead isotopes. The present values are consistently about 100 keV lower than the calculated values, in agreement with the recent measurement of $^{208}\text{Pb}(p, p')$.¹² These results appear to be systematically about 50 keV lower than the earlier measurements,^{8,9} which may reflect differences in over-all beam-energy calibrations. The consistency of the present differences for the lead isotopes suggests that the assumption of a $Z/A^{1/3}$ dependence in the calculations is quite accurate. One should note that the Coulomb energies for ^{206}Pb and ^{209}Bi cannot be obtained from resonance measurements because no suitable target is available.

TABLE I. Coulomb-energy differences.

Isotopes	ΔE_C (MeV) \pm error (keV)	Difference
		$\Delta E_C(\text{obs}) - \Delta E_C(\text{calc})^a$ (keV)
$^{206}\text{Bi}-^{206}\text{Pb}$	18.899 ± 24	-93
$^{207}\text{Bi}-^{207}\text{Pb}$	18.875 ± 28	-85
$^{208}\text{Bi}-^{208}\text{Pb}$	18.816 ± 13	-112
$^{209}\text{Po}-^{209}\text{Bi}$	18.991 ± 12	-146

^a The calculation used the formula $E_C = 1.429Z/A^{1/3} - 0.849$ (MeV) from Long *et al.* (Ref. 13).

It can also be noted from Fig. 3 that the Po-Bi Coulomb-energy difference is even further from the calculated value than the Bi-Pb values. In particular, the difference between our values for ^{209}Bi and ^{208}Pb is 34 ± 18 keV. This difference only depends on the relative measurements for these two targets and is independent of the energy calibration of the beam-analysis system. (The difference is increased if earlier measurements from other laboratories are included.) This difference, although fairly small, is suggestive of a slight effect due to the extra proton in the $h_{9/2}$ shell. According to Nolen and Schiffer,¹⁴ and Auerbach *et al.*,¹⁵ one might expect qualitatively that the macroscopic Coulomb-energy difference is modified by various corrections due to the differences in occupied orbits. However, these differences will also depend inversely on the number of excess neutrons, and therefore small differences are not unexpected.

IV. EXTRACTION OF PARTIAL WIDTHS FOR PROTON DECAY

The cross section for proton emission from the analog state in one channel (\bar{p}) is given by²

$$\frac{d\sigma_{\bar{p}}(E_i, \theta)}{d\Omega} = \frac{\sigma_{pn}(E_i)}{4\pi} f(E_i, \theta) \frac{\Gamma_{\bar{p}}}{\Gamma}, \quad (1)$$

where $\sigma_{pn}(E_i)$ is the total (p, n) cross section to the analog state at bombarding energy E_i . $\Gamma_{\bar{p}}$ is the proton partial width for the observed decay channel and Γ the total width of the level. The function $f(E_i, \theta)$ carries the angular dependence of the decay and is normalized so that $(1/4\pi) \int f(E_i, \theta) d\Omega = 1$. Since the isospin lowering operator (T^-) does not

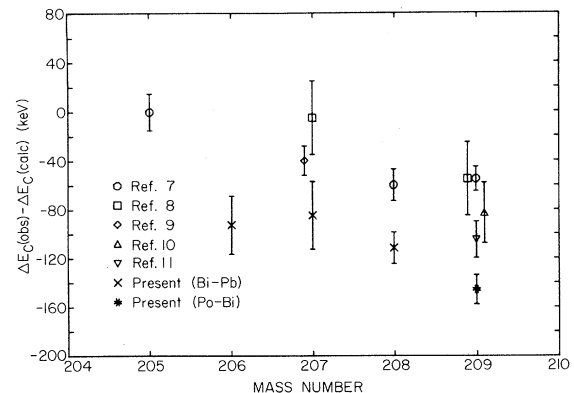


FIG. 3. Coulomb-energy differences. The differences between the observed Coulomb displacement energies and those calculated by Long *et al.* (Ref. 13) are plotted against mass number. All the points plotted are for Bi-Pb Coulomb-energy differences except the one marked Po-Bi for $A = 209$.

alter the population of magnetic substates, the decay of the IAS is expected to be isotropic so that $f(E_i, \theta) = 1$. This has been confirmed for all the observations made so far.² Of course for the 0^+ analog of ^{208}Pb and ^{206}Pb , isotropy is required without any assumption about the nature of the reaction.

The angular dependence of the total cross section for \bar{p} decay for the $^{209}\text{Bi}(p, n\bar{p})$ reaction was measured (Fig. 4) and was found to be isotropic to $\pm 10\%$ as expected. This angular dependence was therefore used in extracting the partial widths.

From Eq. (1) we see that a knowledge of the (p, n) cross section is normally required to extract values of Γ_p/Γ for decay to a particular final state. However, in the lead region, since decays to a number of excited states of the final nucleus are observed, it is possible to obtain the relative proton decay widths independently of the (p, n) cross section. Here the yield for proton decay to a particular final state or multiplet of states of the final nucleus is given by

$$\frac{d\sigma}{d\Omega}(\bar{p}) \propto \sum_i \frac{2j+1}{2T+1} \frac{2P_i(E)\gamma_{pi}^2}{(E-E_i)^2 + \Gamma^2/4}, \quad (2)$$

where, in general, the sum over i is over all members of a multiplet, j is the angular momentum of the emitted proton, and T is the isospin of the IAS. The proton width has been given explicitly in terms of the penetration function $P_i(E)$ and the reduced width γ_{pi}^2 . In terms of the wave number k and the regular and irregular Coulomb wave functions, the penetration function used in the calculations is

$$P_i = kR(F_i^2 + G_i^2)^{-1},$$

evaluated at the radius $R = 7.68$ fm.

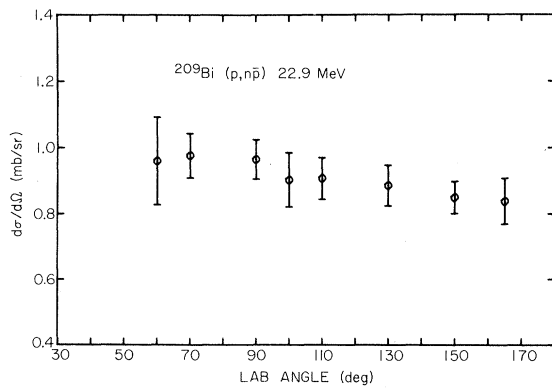


FIG. 4. Angular distribution of the cross section for the sum of all proton decay channels observed ($p_{1/2}$, $f_{5/2}$, and $p_{3/2}$) in the $^{209}\text{Bi}(p, n\bar{p})$ reaction. The absolute normalization is uncertain to $\pm 15\%$.

Corrections to the peak shapes for target thickness and kinematics were also folded into the fitting equation. A smooth background was subtracted from the original experimental spectrum. The remaining spectrum, except for regions obscured by contaminant peaks, was fitted using a least-squares method, searching on the relative reduced widths and gridding on the total width. In the reaction $^{208}\text{Pb}(p, n\bar{p})^{207}\text{Pb}$, the $p_{1/2}^{-1}$, $f_{5/2}^{-1}$, and $p_{3/2}^{-1}$ states are observed. In the reaction $^{209}\text{Bi}(p, n\bar{p})^{208}\text{Bi}$ the corresponding ($\pi h_{9/2}$, $\nu l j^{-1}$) multiplets are seen. Since states are not resolved within a multiplet, one measures only the summed reduced width for the multiplet γ_{ij}^2 . In the fitting we assume that the strength is distributed within a multiplet according to the statistical weight of each state i :

$$\gamma_{pi}^2 = \frac{(2I_i + 1)\gamma_{ij}^2}{10(2j + 1)}.$$

V. RESULTS FOR ^{208}Pb

If the ^{208}Pb core is assumed to be closed, the analog state in ^{208}Bi is simply given by

$$\text{IAS} = \sum_j \left(\frac{2j+1}{45} \right)^{1/2} [\pi l j, (\nu l j)^{-1} | c \rangle,$$

where l, j refer to the shell-model states containing excess neutrons in ^{208}Pb and $|c\rangle$ refers to the (closed) ^{208}Pb core. The proton decays of this analog state lead to the single-neutron-hole states of ^{207}Pb . The results obtained in this case should be directly comparable to those obtained from proton-resonance measurements on ^{207}Pb .

Two spectra taken at different energies, angles, and with different targets are shown in Fig. 5. The

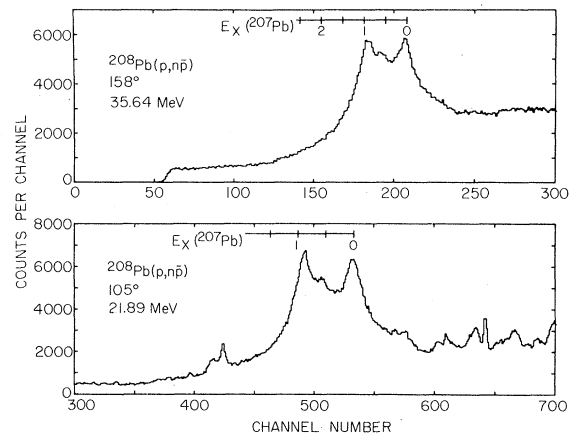


FIG. 5. Proton energy spectra showing the reaction $^{208}\text{Pb}(p, n\bar{p})^{207}\text{Pb}$. Peaks from inelastic scattering on carbon and oxygen contaminants are observed in the lower spectrum.

peaks corresponding to decays to the lowest three hole states in ^{207}Pb are a dominant feature of the spectrum at angles greater than 90° . Decays leading to higher states are inhibited strongly by the barrier and are not observed. The spectrum at 22 MeV was taken with a thinner target than the other spectrum, and the impurity peaks are more pronounced. Two other obvious features are worth noting. First, the width of the peaks is due primarily to the intrinsic width of the analog state, although the width obtained here is even larger than that observed by resonance measurements. The second feature is the noticeable peak corresponding to the 570-keV $f_{5/2}$ hole state which, in spite of the width of the states, shows up between the two major peaks at excitation energies of 0 and 897 keV.

An example of a fit using the method outlined in Sec. IV is shown in Fig. 6. One notices from the fitting that the minimum χ^2 is obtained for widths nearer 340 ± 40 keV rather than the 220 ± 20 -keV total width obtained from the resonance measurements. In fact the best fit with a 220-keV total width has a χ^2 of 27.8 compared with the minimum χ^2 of 1.8 and by eye inspection does not give a satisfactory fit to the data. This is not due to any ex-

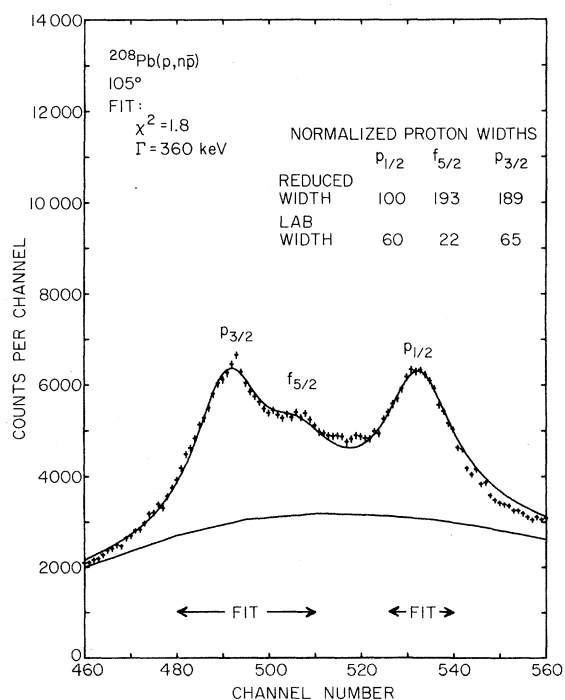


FIG. 6. Proton spectrum showing a fit used to extract total and partial widths. In this example some of the channels between the $p_{1/2}$ and $f_{5/2}$ peaks were omitted in the fitting, as were the tail regions. The widths obtained from this measurements are indicated. (See Table II for averages.)

perimental limit on the resolution from either the detector or the target thickness, as evidenced by the deuteron spectra taken simultaneously with better resolution. Calculations of the kinematic broadening discussed earlier also rule this out as an explanation of the larger width.

The other noticeable feature of the spectrum is that unless the total width is made greater than 380 keV, the theoretical curve underestimates the strength observed in the valley at energies just below the $p_{1/2}$ peak. This feature is common to the fits for ^{209}Bi .⁴ One possible explanation might be that there is an additional small peak in the valley corresponding to \bar{p} decays of an excited analog of, for example, the 3^- , 2.61-MeV state in ^{208}Pb , to the close doublet at about 2.6 MeV in ^{207}Pb . The small energy shift could be due to a different Coulomb-energy difference for the 0^+ and 3^- analogs. This possibility was ruled out by running at a beam energy 460 keV below the expected threshold for excitation of the 3^- analog by the (p, n) reaction. No loss of strength was observed in the valley region (see Fig. 7). This effect and the excess

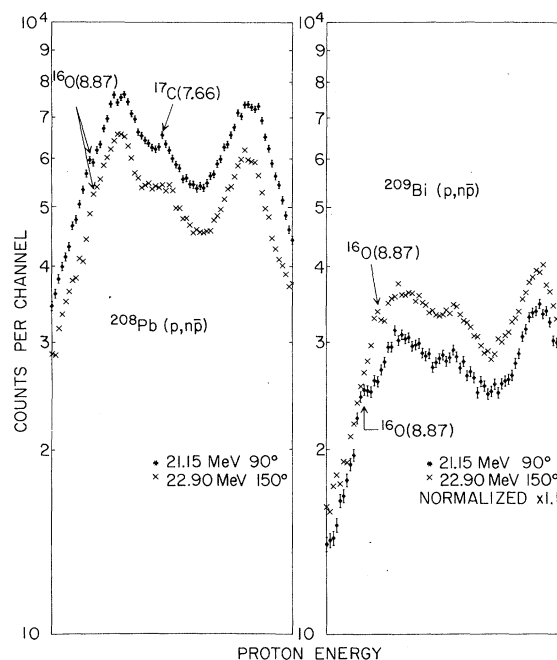


FIG. 7. Comparison of proton spectra above and below the threshold for excited analog-state production in $^{208}\text{Pb}(p, n\bar{p})$. Data obtained using the ^{209}Bi target under the same conditions are also shown, as they are very similar. The scale is semilogarithmic to facilitate comparison of the shapes of the spectra. There is no apparent effect due to crossing the threshold on the depth of the valley. The measurements were made at different angles to avoid interference from contaminant groups. The proton energy scale was translated slightly to compensate for the kinematic shift.

broadening of the \bar{p} lines is unexplained.

The results for ^{208}Pb and ^{209}Bi are shown in Table II, together with comparable results from other experiments. The present results are seen to differ from the $^{207}\text{Pb}(p, p')$ resonance measurements only in the total width of the analog state. The discrepancy there is substantial, however. The analog of ^{209}Bi seems to be very similar to that of ^{208}Pb in its decay properties except that the $f_{5/2}$ channel has substantially more strength in the case of ^{209}Bi . Unfortunately, it is impractical to verify this by the resonance technique because a ^{208}Bi target would be required. A more complete reaction theory may be required for ^{209}Bi , and such a calculation is being made.¹⁶

The experimental reduced widths shown are comparable to the theoretical single-particle values obtained by Andersen, Bondorf, and Madsen¹⁷ for the decay of the IAS in ^{208}Bi which, after renormalization become 100, 89.6, and 109.5 for the $p_{1/2}$, $f_{5/2}$, and $p_{3/2}$ channels, respectively. The single-particle reduced widths were obtained by calculating the total width of each single-particle resonance in a real potential and dividing this by the Coulomb penetration factor P_i evaluated at the resonance energy. The strength of the potential was adjusted to lower the resonance energy enough so that changes in the penetration factor over the width of the resonance were negligible. The reduced widths should be nearly independent of the exact value of the resonance energy in this procedure.

The ratios of the experimental to the theoretical reduced widths are the relative spectroscopic factors. Our data for the decay of the IAS in ^{208}Bi

yield the values 1.0, 0.82, and 0.87 for the $p_{1/2}$, $f_{5/2}$, and $p_{3/2}$ states in ^{207}Pb , respectively. In the absence of a theoretical prediction for the decay of the IAS in ^{209}Po , it is reasonable to compare the same single-particle values with the $^{209}\text{Bi}(p, n\bar{p})$ results. The relative spectroscopic factors, summed over the members of each multiplet in ^{208}Bi , are 1., 1.19, and 0.92 for the $p_{1/2}$, $f_{5/2}$, and $p_{3/2}$ neutron-hole states, respectively.

Nine independent measurements with ^{208}Pb and five with ^{209}Bi were combined in a weighted average to obtain the quoted results. The uncertainty on individual measurements of the total width varied from 55 to 147 keV with most below 90 keV. This uncertainty corresponds to an increase of χ^2 by a factor of 2 above its minimum value, a conservative estimate of the error, since the minimum χ^2 per degree of freedom was generally between 1.0 and 2.5. Errors were assigned, once the optimum parameter values were found, by changing each parameter separately to five different values and recording χ^2 at each point. A parabola was then determined by a least-squares fit to these points, and this function was used to analytically calculate the errors as described above.

Because of the difficulty referred to previously in reproducing the spectrum shape in the valley between the $p_{1/2}$ and $f_{5/2}$ peaks, the data were analyzed both including and excluding the valley region from the fits. The results in Table II correspond to omitting the valley region. When the entire \bar{p} group is fitted one obtains $\Gamma = 351 \pm 24$ keV for ^{208}Pb and $\Gamma = 346 \pm 27$ keV for ^{209}Bi . The relative partial widths are negligibly affected, except for the ^{208}Pb values of $\Gamma_{f_{5/2}}$ and $\gamma_{f_{5/2}}^2$ which become

TABLE II. Total widths and single-particle widths derived from the present analysis and some previous experiments, normalized to facilitate comparison. In the present work the partial proton widths Γ_{ij} are calculated from the reduced widths γ_{ij}^2 , which together with Γ compose the set of fitting parameters (see text). Our quoted errors correspond to an increase of χ^2 above the minimum value by a factor of 2. Errors in the relative proton widths include the contribution from the error of the $p_{1/2}$ width in quadrature.

Parent nuclide	Ref.	Total width Γ (keV)	Relative single-particle partial widths ^a			Relative single-particle reduced widths ^b		
			$\Gamma_{p_{1/2}}$	$\Gamma_{f_{5/2}}$	$\Gamma_{p_{3/2}}$	$\gamma_{p_{1/2}}^2$	$\gamma_{f_{5/2}}^2$	$\gamma_{p_{3/2}}^2$
^{208}Pb	This work	317 ± 24	60	25.2 ± 1.9	65.6 ± 2.4	100	73.5 ± 5.7	95.6 ± 3.5
	17	220	60	17	40			
	8	220 ± 20	60	17 ± 6	49 ± 16			
	3	...	60	21.3 ± 2.6	68.5 ± 4.0			
	c	220 ± 20	60	27 ± 3	68.5 ± 5			
^{209}Bi	This work	327 ± 31	60	36.1 ± 2.9	68.3 ± 3.8	100	107 ± 9	101 ± 6
	4	380 ± 80	60	43 ± 5	67 ± 5			

^a Normalized to make $\Gamma_{p_{1/2}} = 60$.

^b Normalized to make $\gamma_{p_{1/2}}^2 = 100$.

^c These values were quoted in Ref. 18 as a private communication from von Brentano *et al.*

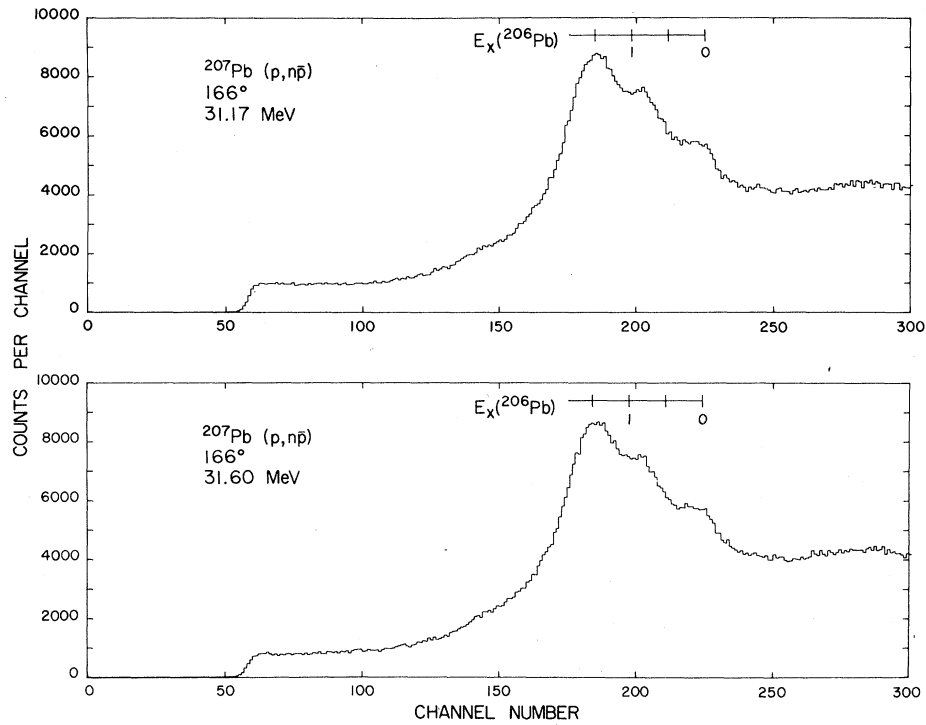


FIG. 8. Proton energy spectra showing the reaction $^{207}\text{Pb}(p, n\bar{p})^{206}\text{Pb}$.

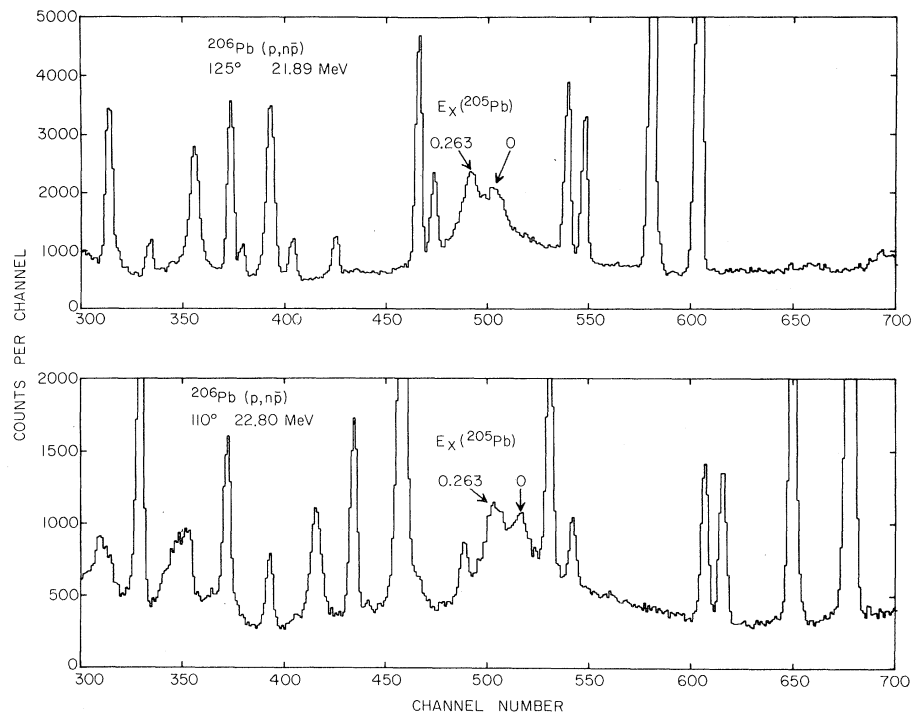


FIG. 9. Proton spectra showing the $^{206}\text{Pb}(p, n\bar{p})^{205}\text{Pb}$ reaction. The two \bar{p} groups observed are labeled with the corresponding excitation energy in the residual nucleus. The numerous other large peaks are due to the $^{12}\text{C}(p, p')$ and $^{16}\text{O}(p, p')$ reactions.

20.8 ± 2.2 and 170 ± 19 , respectively. The change is only slightly outside of the quoted uncertainty.

One might speculate on the possible explanations for the discrepancy in the total width. First, the uncertainty may be underestimated in one or more measurements. It does not seem very likely that a large source of broadening could have been overlooked in our analysis. One difficulty is assigning the background to be subtracted from the proton spectrum. We assumed a smooth background, qualitatively like an evaporation spectrum, in our analysis. A peak from a (p, p') reaction could accidentally fall inside the \bar{p} group at one bombarding energy and detection angle, but the consistency of the results at a number of energies makes this possibility unlikely as an explanation for the large widths that are found. Similarly, the resonance measurements have been performed independently a number of times and show consistency.

A second possibility is that the discrepancy might be a manifestation of the spreading of the analog configuration caused by charge-dependent forces. In all analyses of data performed so far, one has fitted a single-level line shape to the envelope of numerous unresolved and presumably overlapping levels. The effect of interference on

the line shape in the $(p, n\bar{p})$ reaction could very well differ from that in the compound (p, p') reaction, depending on the structure of the states that are mixed with the analog state. The possibility of observing such differences has been referred to previously.^{2,9}

Finally, it is interesting to note that the calculations by Bund and Blair¹⁸ of the total width of the ^{208}Pb analog state in an optical-model formalism give values ranging from 277 to 629 keV, all larger than the 220-keV measured value from the $^{207}\text{Pb}(p, p')$ reaction.

VI. RESULTS FOR ^{207}Pb

Proton decays from the reaction $^{207}\text{Pb}(p, n\bar{p})^{206}\text{Pb}$ are shown in Fig. 8. The unusual width of the peaks noted in the ^{206}Pb spectrum is even more noticeable in this case. The ground state and first excited state of ^{206}Pb are 803 keV apart, but the ground state shows up only as a shoulder on the high-proton-energy side. The largest peak corresponds to decays to the group of states between 1.17 and 1.78 MeV, the peak occurring at an excitation energy of 1.42 MeV. Because of the many states included and the unusual width of the peaks, no significant fits to the ^{207}Pb data were obtained. The total width inferred from fits to the two "isolated" peaks corresponding to the 0- and 803-keV states in ^{206}Pb is 540 keV, but this number should be regarded only as an indication that the assumed simple form for the line shape does not apply to this analog state. The best fit is very poor ($\chi^2 = 12$). This is not because the data are ambiguous or marginal. Every measurement of the $^{207}\text{Pb}(p, n\bar{p})$ spectrum has the same shape as those in Fig. 8. The width of the $p_{1/2}$ ground-state analog resonance has been measured in a $^{206}\text{Pb}(p, p')$ experiment^{8,19} as 170 keV, which is much smaller than any reasonable value extracted from the \bar{p} spectrum. This is an even greater discrepancy than was observed in the $^{208}\text{Pb}(p, n\bar{p})$ case and is a clear indication that the analog state exhibits different spectral distributions in the two reactions.

VII. RESULTS FROM ^{206}Pb

In contrast to the broad peaks observed for ^{207}Pb , the decay proton groups from the IAS in ^{206}Bi are very narrow (Fig. 9). The total width of the IAS is found to be 230 ± 38 keV. The ^{206}Pb target contained more carbon and oxygen than the other targets so that a careful selection of bombarding energy and angle had to be made to avoid overlap between the \bar{p} peaks and proton groups due to the contaminants.

The spectrum of ^{205}Pb consists of a $(\frac{5}{2}^-)$ ground state, a $(\frac{1}{2}^-)$ 2.3-keV first excited state, and a $(\frac{3}{2}^-)$

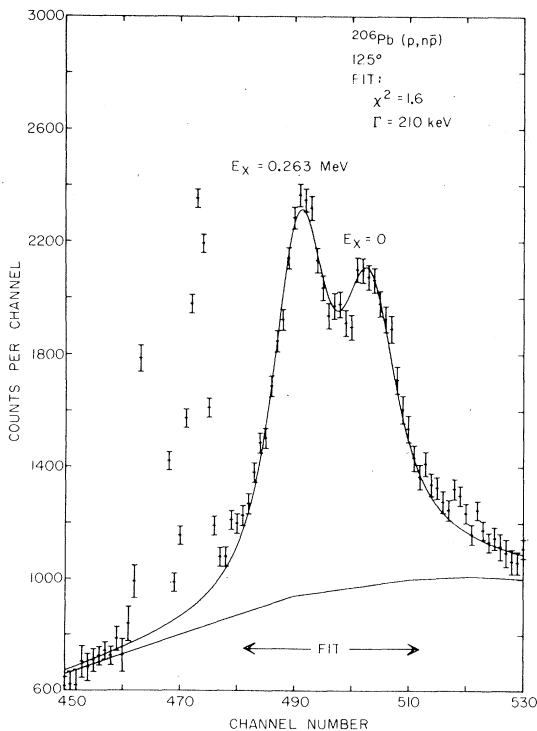


FIG. 10. Proton spectrum for $^{206}\text{Pb}(p, n\bar{p})$ showing a typical fit. The contaminant peaks between channels 460 and 480 were excluded from the fit, as indicated on the figure.

second excited state at 0.263 MeV.²⁰ Proton decays to higher states are not observed, and the ground-state doublet is impossible to resolve in this experiment because of the width of the analog state. If ²⁰⁶Pb had no occupation in the $p_{1/2}$ neutron shell, one would expect no population of the $\frac{1}{2}^-$ state by the \bar{p} decay of its analog. If, in order to extract relative decay widths we assume this, and also that the $p_{3/2}$ and $f_{5/2}$ neutron orbitals in ²⁰⁶Pb were fully occupied, we find a value for $\Gamma_{f_{5/2}}$ of 67 ± 7 and for $\gamma_{f_{5/2}}^2$ of 212 ± 23 , relative to the normalizations making $\Gamma_{p_{3/2}}$ and $\gamma_{p_{3/2}}^2$ equal to 100, respectively (Fig. 10). This ratio $\gamma_{f_{5/2}}^2/\gamma_{p_{3/2}}^2$ is thus twice as large for ²⁰⁶Pb as for ²⁰⁸Pb, although the extreme assumptions used make this conclusion less reliable. The wave function of ²⁰⁶Pb does not actually have such a zero-order shell-model structure,²¹ but more detailed calculations were not felt to be justified at this point.

VIII. CONCLUSIONS

The $(p, n\bar{p})$ reaction is a useful and complementary technique to resonance measurements for obtaining widths and Coulomb energies, not only because it gives an alternative method of measuring these properties for the same nuclei studied in the resonance measurements but also because it enables the measurements to be extended to differ-

ent nuclei.

For the analog of ²⁰⁸Pb the partial widths agree reasonably well with those measured in previous resonance work, especially the most recent measurements,¹⁸ whereas the total width found in the $(p, n\bar{p})$ reaction appears to be much larger. The total width found by $(p, n\bar{p})$ for the ²⁰⁹Bi analog is practically the same as that measured for ²⁰⁸Pb. The partial width for the $f_{5/2}$ proton decay mode, however, appears to be significantly different in these two nuclei. The ²⁰⁷Pb analog line shape is much broader than all of the other cases studied and therefore seems to be anomalous. Also the shape of the spectrum evidently cannot be reproduced by the type of calculation in which corrections for penetrability variations, kinematics, and instrumental effects are applied to a single level expression representing the spectral distribution of the analog state.

ACKNOWLEDGMENTS

The authors would like to thank Dr. D. Bayer and W. Wagner for assistance with the data taking and analysis, and Professor G. Bertsch and Professor W. Benenson for valuable comments and discussion.

†Work supported in part by the National Science Foundation.

¹A. I. Yavin, R. A. Hoffswell, L. H. Jones, and T. M. Noweir, *Phys. Rev. Letters* **16**, 1049 (1966).

²P. S. Miller and G. T. Garvey, *Nucl. Phys.* **A163**, 65 (1971).

³G. J. Igo, C. A. Whitten, Jr., J.-L. Perrenoud, J. W. Verba, T. J. Woods, J. C. Young, and L. Welch, *Phys. Rev. Letters* **22**, 724 (1969).

⁴G. M. Crawley, W. Benenson, P. S. Miller, D. L. Bayer, and R. St. Onge, *Phys. Rev. C* **2**, 1071 (1970).

⁵In this paper we will use the term isobaric analog state to refer exclusively to the lowest-energy state with isospin T equal to $T_Z + 1$, that is, the analog of the ground state of the parent nuclide.

⁶T. J. Woods, G. J. Igo, C. A. Whitten, W. Dunlop, and G. W. Hoffmann, *Phys. Letters* **34B**, 594 (1971); and private communication.

⁷E. Kashy, private communication (to be published).

⁸G. H. Lenz and G. M. Temmer, *Nucl. Phys.* **A112**, 625 (1968).

⁹C. D. Kavaloski, J. S. Lilley, P. Richard, and N. Stein, *Phys. Rev. Letters* **16**, 807 (1966).

¹⁰G. M. Temmer, in *Proceedings of the International Conference on Nuclear Physics, Gallinburg, Tennessee, 12-17 September 1966*, edited by R. L. Becker and

A. Zucker (Academic, New York, 1967), p. 223.

¹¹S. A. A. Zaidi, J. L. Parish, J. G. Kulleck, C. F. Moore, and P. von Brentano, *Phys. Rev.* **165**, 1312 (1968).

¹²P. von Brentano, W. K. Dawson, C. F. Moore, P. Richard, W. Wharton, and H. Wieman, *Phys. Letters* **26B**, 666 (1968); W. R. Wharton, P. von Brentano, W. K. Dawson, and P. Richard, *Phys. Rev.* **176**, 1424 (1968).

¹³D. D. Long, P. Richard, C. F. Moore, and J. D. Fox, *Phys. Rev.* **149**, 906 (1966).

¹⁴J. A. Nolen, Jr., and J. P. Schiffer, *Ann. Rev. Nucl. Sci.* **19**, 471 (1969).

¹⁵N. Auerbach, J. Hufner, A. K. Kerman, and C. M. Shakin, *Phys. Rev. Letters* **23**, 484 (1969).

¹⁶A. Kromminga, private communication.

¹⁷B. L. Andersen, J. B. Bondorf, and B. S. Madsen, *Phys. Letters* **22**, 651 (1966).

¹⁸G. W. Bund and J. S. Blair, *Nucl. Phys.* **A144**, 384 (1970).

¹⁹N. Stein, C. A. Whitten, and D. A. Bromley, *Phys. Rev. Letters* **20**, 113 (1968).

²⁰C. M. Lederer, J. M. Hollander, and I. Perlman, *Table of Isotopes* (Wiley, New York, 1968), 6th ed.

²¹W. W. True and K. W. Ford, *Phys. Rev.* **109**, 1675 (1953); V. N. Guman, Y. I. Kharitonov, L. A. Sliv, and G. A. Sogomonova, *Nucl. Phys.* **28**, 192 (1961).